Raman Spectroscopy and Optical Coherence Tomography on a Chip

N. Ismail, B. I. Akca, L. Chang, K. Wörhoff, R. M. de Ridder, and M. Pollnau

Miniaturization of optical instruments for biomedical applications requires the development of efficient means to deliver excitation light to – and collect the resulting signals from – biomedical tissue by an optical microchip, as well as spectral analysis of the acquired information on the chip. We have investigated light collection by integrated waveguides, invented a method for on-chip confocal light delivery and collection, proposed new designs and developed high-resolution arrayed-waveguide gratings (AWGs), and demonstrated Raman spectroscopy and spectral-domain optical coherence tomography (OCT) on a chip.

1. Arrayed waveguide gratings in silicon oxynitride

We developed different AWG spectrometers in silicon oxynitride technology. A new lay-out of the AWG allows the use of equal bends in all arrayed waveguides, thereby greatly facilitating the design of AWGs [1]. Furthermore, we designed and fabricated high-resolution AWGs operating around 800 nm and 1300 nm [2], a broad-spectral-range synchronized flat-top arrayed-waveguide grating applied in a 225-channel cascaded spectrometer [3], and a flat-focal-field integrated spectrometer using a field-flattening lens [4].

2. Confocal light delivery and detection

In a semi-analytical model [5] and Monte-Carlo simulations [6], the light collection efficiency of integrated waveguide probes was compared to that of different types of fiber probes for different thicknesses of weakly and highly scattering samples, respectively. The simulation results show that integrated probes have a collection efficiency that is higher than that of small-core fiber probes, and, in the particular case of thin samples, also exceeds the collection efficiency of large-core, highly multimode fiber probes. An integrated waveguide probe was fabricated and applied to excite and collect luminescence from a Ruby rod [5] and a highly scattering water suspension of latex nanospheres [6]. Experimental and calculated results are in good agreement with each other.

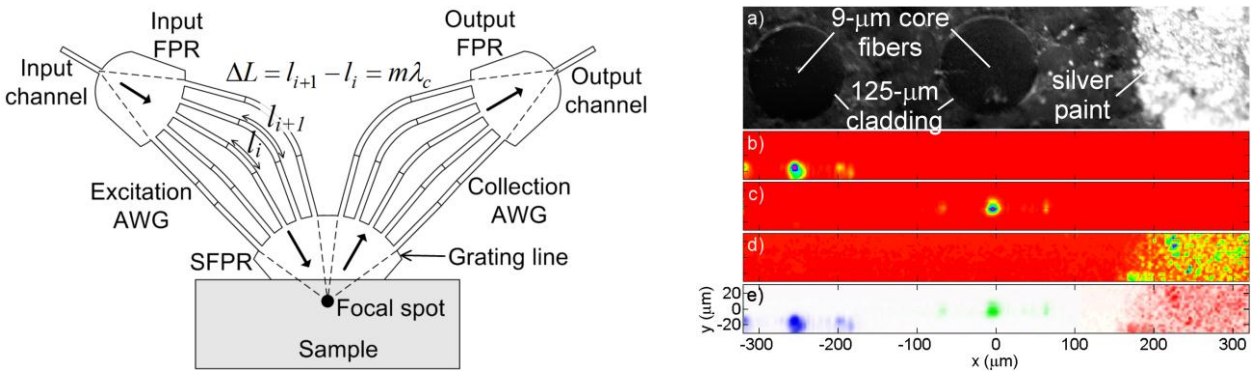

Fig. 1. Confocal arrangement of two AWGs allowing efficient illumination of, and signal collection from, a small focal volume below the sample surface: (left) schematic [7]; (right) spectral imaging: (a) 9-μm fiber array used as a sample; (b)-(d) measurement from output channels centered at 831 nm, 841 nm, and 856 nm; (e) resulting multi-wavelength image [7].

We presented a novel on-chip sensor, based on the confocal arrangement of two AWGs (Fig. 1, left), acting as focusing illuminator and signal collector, respectively [7]. The chip can be close to, or in direct contact with a sample, e.g. biological tissue, without the need of external optics. The collection efficiency of our device can be more than an order of magnitude higher than that of a standard AWG in which light is collected by one input channel. Experimental results on the collection efficiency and volume were obtained, together with a demonstration of multi-wavelength imaging (Fig. 1, right).

3. Raman spectroscopy on a micro-chip

An AWG was applied to Raman spectroscopy (Fig. 2, left). It was validated by reproducing the well-known spectrum of cyclohexane (Fig. 2, right) [8,9]. Subsequently, polarized Raman spectra were measured of extracted human teeth containing localized initial carious lesions [8]. Excellent agreement was obtained between the spectra of healthy and carious tooth enamel measured with our integrated device and spectra recorded using a conventional Raman spectrometer.

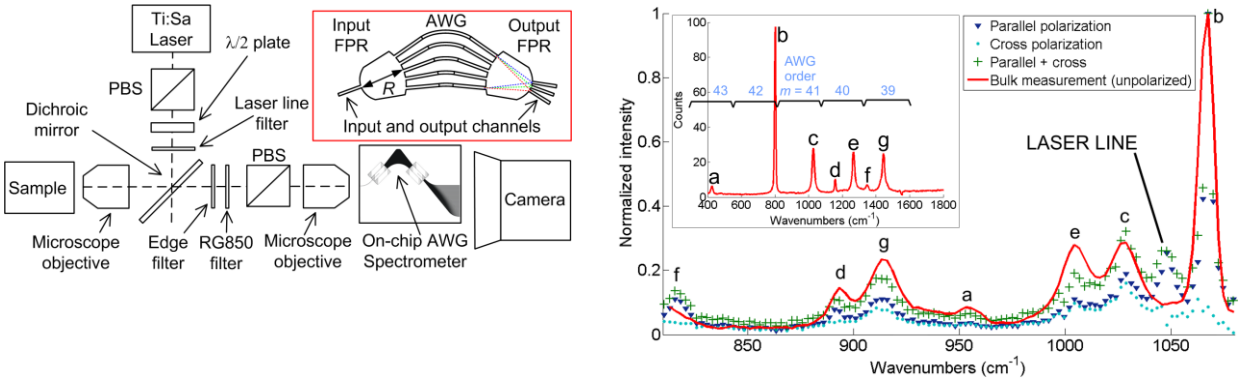

Fig. 2. Setup used for the polarized Raman experiments. Inset: schematic of arrayed waveguide grating (AWG). Normalized Raman spectra of cyclohexane for parallel (triangles) and cross (dots) polarization, measured with the AWG spectrometer; normalized sum of the two spectra (crosses). Unpolarized Raman spectrum (red line) measured with a conventional spectrometer, folded into diffraction order m = 41 of the AWG. Inset: original unfolded spectrum, extending over diffraction orders m = 39, 40, 41, 42, and 43 of the AWG. The individual Raman peaks in both, folded and unfolded spectrum, are assigned by letters (a–g). [8].

4. *In vivo* optical coherence tomography on a micro-chip

AWGs at 800 nm and 1300 nm were inserted into a spectral-domain optical coherence tomography (SD-OCT) system. Interferometric distance measurements were performed using broadband light sources launched into a free-space Michelson interferometer with its output coupled into the AWG. A maximum imaging depth of 1 mm and axial resolutions of 25 μm and 20 μm in air were demonstrated for 800 nm and 1300 nm, respectively [2]. When removing the output channels from the AWG and focusing directly onto a line-scan camera, the imaging depth was improved to 3.3 nm and 4.3 mm at 800 nm and 1300 nm, respectively [10]. Also polarization-independent performance has been demonstrated [10]. OCT measurements were performed and demonstrated imaging up to a maximum depth of 1 mm with an axial resolution of 19 μm, both in agreement with the AWG design parameters. Using the AWG spectrometer combined with a fiber-based SD-OCT system, we demonstrated cross-sectional OCT imaging of a multi-layered scattering phantom [11].

With a spectrometer comprising an arrayed-waveguide grating with 136-nm free spectral range and 0.21-nm wavelength resolution and a beam splitter realized by a non-uniform adiabatic coupler

with its 3-dB splitting ratio being nearly constant over 150 nm (Fig. 3), we demonstrated high-quality *in vivo* imaging in human skin with 1.4-mm penetration depth, 7.5-µm axial resolution, and a signal-to-noise ratio of 74 dB (Fig. 4) [12]. Considering the reasonable performance of this early OCT on-a-chip system and the anticipated improvements in this technology, a completely different range of devices and new fields of applications may become feasible.

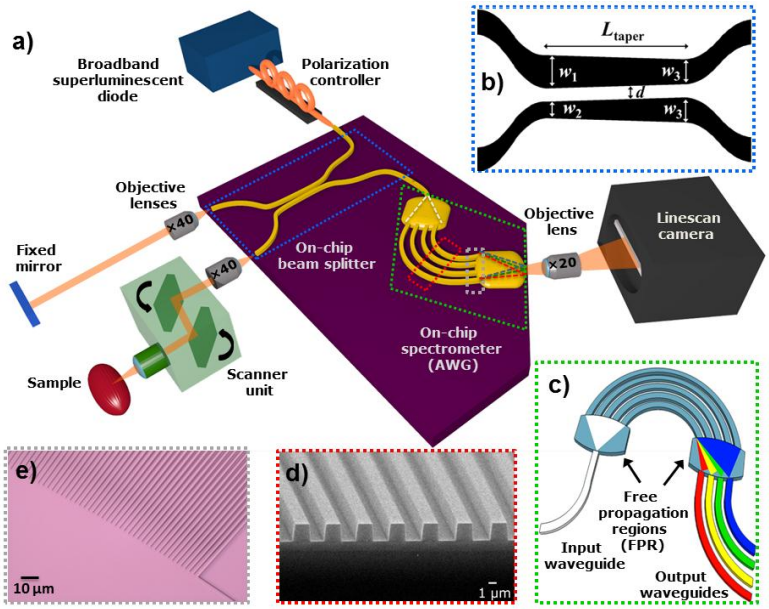

Fig. 3. Schematic of the partially integrated SD-OCT system. **(a)** The complete SD-OCT set-up comprising a broadband light source, the microchip with its optical circuitry consisting of a broadband beam splitter and the spectrometer (purple plate, magnified for viewing purposes), line-scan camera, and reference and sample arms, the latter including a scanner unit. **(b)** Details of the integrated broadband beam splitter. **(c)** A conventional AWG which, in contrast to our device, includes output channels. **(d)** Scanning electron microscope image of the arrayed-waveguide section of the AWG before top-cladding deposition. **(e)** Optical microscope image of linear tapers at the waveguide/FPR interface of the fabricated AWG spectrometer [12].

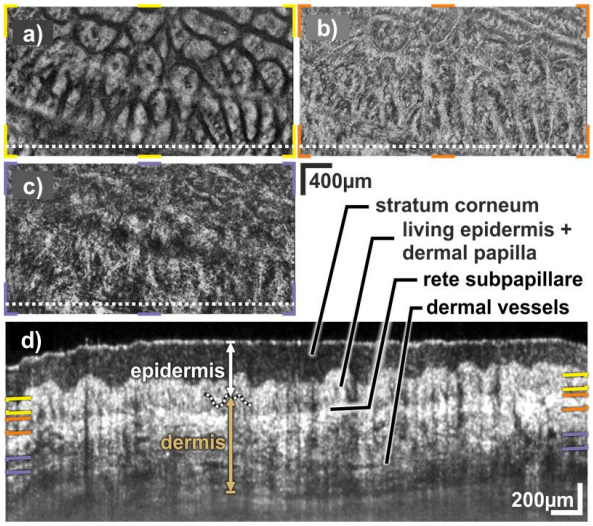

Fig. 4. Images of glabrous skin at interdigital joint taken using the partially integrated SD-OCT system. *En face* section at **(a)** the deeper epidermal layers featuring the living epidermis on top of the dermal papillae (yellow), **(b)** rete subpapillare where fibrous components dominate the basis of the dermal papillae (orange) and **(c)** the deeper dermis with vessels (violet). **(d)** Cross-section as indicated by the dotted white line in the *en face* sections. Colored indicators depict the location of the *en face* views [12].

Collaborations

1. Center for Optical Diagnostics and Therapy, Department of Dermatology, Erasmus Medical Center Rotterdam, The Netherlands.
2. River Diagnostics BV, Rotterdam, The Netherlands.
3. Academic Medical Center, University of Amsterdam, The Netherlands.
4. Biomedical Photonic Imaging Group, University of Twente, The Netherlands.

References

[1] N. Ismail, F. Sun, G. Sengo, K. Wörhoff, A. Driessen, R.M. de Ridder, and M. Pollnau, *"Improved arrayed-waveguide-grating layout avoiding systematic phase errors"*, Opt. Express **19** (9), 8781-8794 (2011).

[2] B.I. Akca, V.D. Nguyen, J. Kalkman, N. Ismail, G. Sengo, F. Sun, A. Driessen, T.G. van Leeuwen, M. Pollnau, K. Wörhoff, and R.M. de Ridder, *"Toward spectral-domain optical coherence tomography on a chip"*, IEEE J. Sel. Top. Quantum Electron. **18** (3), 1223-1233 (2012).

[3] B.I. Akca, C.R. Doerr, G. Sengo, K. Wörhoff, M. Pollnau, and R.M. de Ridder, *"Broad-spectral-range synchronized flat-top arrayed-waveguide grating applied in a 225-channel cascaded spectrometer"*, Opt. Express **20** (16), 18313-18318 (2012).

[4] B.I. Akca, G. Sengo, M. Pollnau, A. Driessen, K. Wörhoff, and R.M. de Ridder, *"Flat-focal-field integrated spectrometer using a field-flattening lens"*, Opt. Lett. **37** (20), 4281-4283 (2012).

[5] N. Ismail, F. Civitci, K. Wörhoff, R.M. de Ridder, M. Pollnau, and A. Driessen, *"Efficiency of integrated waveguide probes for the detection of light backscattered from weakly scattering media"*, Appl. Opt. **50** (6), 935-942 (2011).

[6] N. Ismail, F. Sun, K. Wörhoff, A. Driessen, R.M. de Ridder, and M. Pollnau, *"Excitation and light collection from highly scattering media with integrated waveguides"*, IEEE Photon. Technol. Lett. **23** (5), 278-280 (2011).

[7] N. Ismail, B.I. Akca, F. Sun, K. Wörhoff, R.M. de Ridder, M. Pollnau, and A. Driessen, *"Integrated approach to laser delivery and confocal signal detection"*, Opt. Lett. **35** (16), 2741-2743 (2010).

[8] N. Ismail, L.P. Choo-Smith, K. Wörhoff, A. Driessen, A.C. Baclig, P.J. Caspers, G.J. Puppels, R.M. de Ridder, and M. Pollnau, *"Raman spectroscopy with an integrated arrayed-waveguide grating"*, Opt. Lett. **36** (23), 4629-4631 (2011).

[9] A.C. Baclig, N. Ismail, K. Wörhoff, A. Driessen, R.M. de Ridder, M. Pollnau, P.J. Caspers, and G.J. Puppels, *"Arrayed-waveguide-grating approach for wavelength selection in Raman spectroscopy"*, J. Raman Spectrosc. **43** (9), 1306-1311 (2012).

[10] B.I. Akca, L. Chang, G. Sengo, K. Wörhoff, R.M. de Ridder, and M. Pollnau, *"Polarization-independent enhanced-resolution arrayed-waveguide grating used in spectral-domain optical low-coherence reflectometry"*, IEEE Photon. Technol. Lett. **24** (10), 848-850 (2012).

[11] V.D. Nguyen, B.I. Akca, K. Wörhoff, R.M. de Ridder, M. Pollnau, T.G. van Leeuwen, and J. Kalkman, *"Spectral domain optical coherence tomography imaging with an integrated optics spectrometer"*, Opt. Lett. **36** (7), 1293-1295 (2011).

[12] B.I. Akca, B. Považay, A. Alex, K. Wörhoff, R.M. de Ridder, W. Drexler, and M. Pollnau, *"Miniature spectrometer and beam splitter for an optical coherence tomography on a silicon chip"*, Opt. Express **21** (14), 16648-16656 (2013).